

A Heat Transfer Comparison between a Synthetic Jet and a Steady Jet at Low Reynolds Numbers

Rayhaan Farrelly

Mechanical Engineering Dept., Trinity College
Dublin 2, Ireland, farrelra@tcd.ie

Tim Persoons

Mechanical Engineering Dept., Trinity College
Dublin 2, Ireland

Alan McGuinn

Mechanical Engineering Dept., Trinity College
Dublin 2, Ireland

Darina B. Murray

Mechanical Engineering Dept., Trinity College
Dublin 2, Ireland

ABSTRACT

A study has been carried out to compare steady jet and synthetic jet heat transfer distributions at low Reynolds numbers. Both jets issued from a 5mm diameter orifice plate with air for the steady jet being supplied by a compressor via a plenum chamber. Tests were conducted for Reynolds numbers ranging from 1000 to 4000, and for non-dimensional surface to jet exit spacings (H/D) from 1 to 6. Dimensionless stroke length (L_o/D) for the synthetic jet was held constant at 8. A significant difference was observed between the steady and synthetic jet Nusselt numbers at low Reynolds numbers and low H/D . In comparison to steady jets, the stronger entrainment of surrounding fluid and the vigorous mixing near the impingement surface are characteristics of synthetic jets that are beneficial to heat transfer. Nonetheless, the steady jet yields higher Nusselt numbers for all test conditions.

INTRODUCTION

The use of synthetic jets for cooling of electronics is a relatively new technology which has shown great promise in a number of practical applications. It is well established that effective rates of cooling can be achieved using conventional steady flow impinging jets.

More recently it has been shown by Kercher et al. (2003) that synthetic jets can deliver similar cooling effects without the need for an external air supply system. In a review article by Glezer and Amitay (2002), it was noted that impinging synthetic jets are proving to be an extremely promising technology for use in electronics cooling and also have excellent potential for cooling in manufacturing processes.

A synthetic jet is a fluid motion generated by sufficient strong oscillatory flow at a sudden expansion. Although synthetic jets have potential for many cooling applications, it is

however a particularly attractive candidate for cooling miniature surfaces, like electronic packages, because they can affect the heat transfer on extremely small scales and enhance the transport and mixing of the heated fluid.

The primary advantage of the synthetic jet is its zero-net-mass flux nature, which eliminates the need for plumbing, and, when applied to a base flow (one of the primary uses for synthetic jets is in vectoring a main steady flow) results in unique effects not possible with steady or pulsed suction or blowing. The synthetic jet can easily be integrated into complex geometries, requires relatively low operating power, is simple to design and fabricate, and unlike traditional fans or steady jets, it does not require external ducting.

Recently, the question of how a synthetic jet would compare to a steady jet at the same Reynolds number has received some attention. Previous experiments by Smith and Glezer (1998) have shown that a low Reynolds number synthetic jet has many characteristics that are similar to steady jets at a higher Reynolds number.

The purpose of this study is to acquire an understanding of how synthetic jets compare with and differ from steady jets at matched Reynolds numbers, and to investigate the effects of some of the dimensionless parameters of synthetic jets.

The experimental apparatus and measurement techniques are described next, followed by the results of the comparison between the synthetic jet and steady jet

NOMENCLATURE

D	Jet diameter, m
h	Convective heat transfer co-efficient W/m^2K
H	Height of nozzle above plate, m
k	Thermal conductivity, W/mK
k_s	Thermal conductivity of sensor barrier, W/mK
L_o	Jet's stroke length, m
Nu	Nusselt number, based on D and jet temperature
Pr	Prandtl number
\ddot{q}	Heat flux, W/m^2
r	Radial distance along plate from geometric centre, m
Re	Reynolds number, based on D
ΔT	Temperature difference, $^{\circ}C$
U_o	Average jet velocity, m/s
δ	Sensor thickness, m
ν	Kinematic viscosity, m^2/s

EXPERIMENTAL SETUP

Bearing in mind that this study is focusing on two different types of jets, there are three main elements that make up the experimental rig, these being the synthetic jet, the steady jet and the heated impingement surface.

The impingement surface and both jets are mounted on independent carriages that travel on orthogonal tracks; the carriage for the impingement surface is moved using a computer controlled traverse.

The carriage for the jets is moved using a manually operated lead screw actuator. The instruments associated with the heated impingement surface are two single point heat flux sensors and two thermocouples.

The rig designs for the synthetic jet and the steady jet respectively are presented in figure 1a and figure 1b.

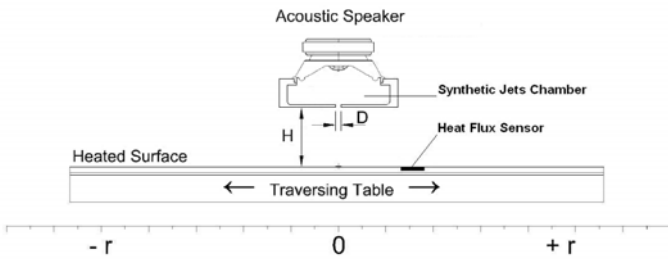


Figure 1a: Schematic of the synthetic jet test apparatus

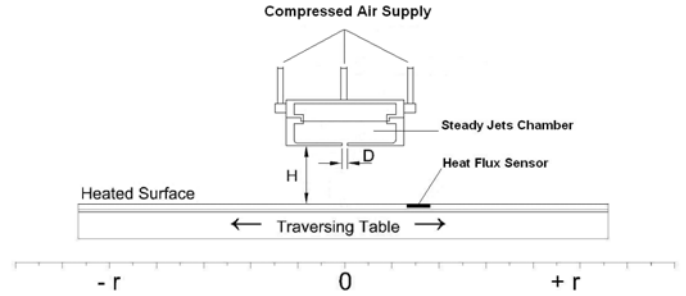


Figure 1b: Schematic of the steady jet test apparatus

The operation of the synthetic jet relies primarily on an acoustic speaker mounted on an enclosed cavity with an orifice plate on the opposing side to provide the entrainment path for the working fluid. The speaker is a Visaton[®] FR8 audio speaker. A signal input is required to control the driving frequency of the speaker; this is provided by a TTi TG315 Signal Generator, and the signal is amplified using a Kemo[®] 40 Watt power amplifier. The speaker was supplied with a sinusoidal wave of specific amplitude and frequency so as to obtain the desired stroke length and Reynolds number. The use of a loudspeaker allows for a more continuous range of driving frequencies than has been achieved in the past.

The cavity body and orifice plate are constructed from a thermoplastic and were fabricated using a method of rapid prototyping called fused deposition modelling. The cavity has an approximate volume of $100cm^3$ with an orifice diameter of 5mm. The synthetic and steady jets were clamped onto a carriage, which allows for height adjustment from 1 to 6 diameters above the impingement surface. The jets are fixed at a normal angle of impingement (90°).

An impinging synthetic jet flow is characterised by three parameters: The surface to orifice spacing H/D , the dimensionless stroke length L_o/D and the Reynolds number $Re = U_o D/\nu$, where $L_o = \int_0^{T/2} U(t) dt$, T is the oscillation period, $U_o = L_o/(T/2)$ and $U(t)$ is the area-averaged orifice velocity. L_o/D is inversely proportional to a Strouhal number, since $L_o/D = \frac{1}{2}(f D/U_o)^{-1}$. The synthetic jet operating point is set using a semi-empirical relationship between the cavity pressure and jet velocity with an orifice damping coefficient $K = 1.459$ Persoons and O'Donovan (2007).

The steady jet was formed from a constant compressed air source that was maintained at flow rates corresponding to jet Reynolds numbers ranging from 1000 to 4000 by an MKS[®] Instruments 1579A Digital Mass Flow Controller, which has an accuracy of 1% of full scale and a repeatability of $\pm 0.2\%$ of full scale (300 slm). In order to maintain a steady flow to the mass flow controller, two pressure regulators with one acting as

a slave regulator, combined with a plenum chamber, were utilised. The jet impinges onto a surface that consists of a 5mm thick flat copper plate measuring 425mm x 550mm. To the underside of the plate a silicon rubber heater mat is glued with a thin layer of adhesive. The mat is approximately 1.1mm thick. The underside of the plate and mat assembly is insulated from the surroundings. The entire assembly is such that it approximates a uniform wall temperature boundary condition. The system is typically operated at a surface temperature of 40°C.

The sensor utilised in this study is an RdF Micro-Foil® heat flux sensor. The heat flux sensor is mounted flush with the surface of the plate; to achieve this it was necessary to embed the sensor in the plate by machining a groove in the surface and gluing it down using a thermally conductive epoxy. The sensor is positioned centrally on the plate, and together with the jet and plate carriage arrangement, allow for heat transfer measurements beyond 20 diameters from the geometric centre of the jet. In this study, testing has only been concerned within the region of 1 to 6 diameters from the geometric centre of the jet. The Micro-Foil® heat flux sensor measures the temperature differential across a known thermal barrier using a differential thermopile. The heat flux through the sensor is based on the following equation:

$$\ddot{q} = k_s \frac{\Delta T}{\delta} \quad (1)$$

Where ΔT is the temperature difference across the thickness (δ) of the barrier and k_s is the thermal conductivity of the barrier (kapton). A single pole T-type thermocouple is also embedded in this sensor to measure the local temperature.

The Micro-Foil® heat flux sensor was calibrated using a nozzle with a diameter of 13mm. The stagnation point heat transfer was used for the calibration of the Micro-Foil® sensor. By comparison against the following correlation from Liu and Sullivan (1996), Liu and Sullivan (1996) have shown that at low $H / D (< 2)$ the convective heat transfer coefficient is constant and independent of nozzle height above the impingement surface, has shown to hold true for Re between 10000 and 30000

$$0.585 = \frac{Nu_{stag}}{Pr^{0.4} Re^{0.5}} \quad (2)$$

The voltage produced by the Micro-Foil® heat flux sensor was recorded when the sensor was placed at the stagnation point under the impinging jet. The height of the nozzle above the heated impingement surface was 0.75D. The Reynolds number was varied from 10000 to 30000. The calculated heat

flux was plotted against the voltage produced under the test conditions, which produced an R^2 value of 0.9975. The Nusselt number $Nu = hD/k$ is determined with the jet temperature as a reference. The heat transfer rig used in this paper is similar to that used by O'Donovan and Murray (2007).

The mean Nusselt number has a calculated uncertainty of 5.7%. This uncertainty is based on a worst case scenario where the uncertainty is a percentage of the smallest measurements. A complete calibration and uncertainty analysis for this experimental set-up is reported by O'Donovan and Murray (2007).

The experiments were repeated several times to ensure repeatability of the results.

RESULTS AND DISCUSSION

Figures 2 through 4 illustrate the heat transfer profiles for the synthetic jet and steady jet at three different H/D values of 1, 2 and 6, and four different Reynolds numbers ranging from 1000 to 4000 for both jets.

A comparison between the heat transfer profiles and features of synthetic jets and steady jets will be covered in this section.

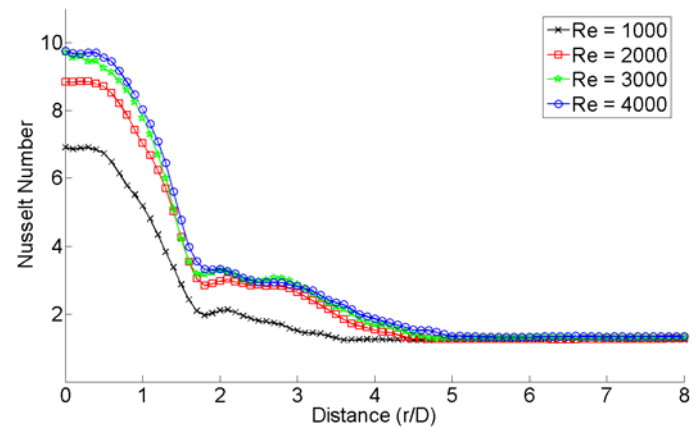


Figure 2a: Heat transfer distribution for a synthetic jet at $H/D = 1.0$

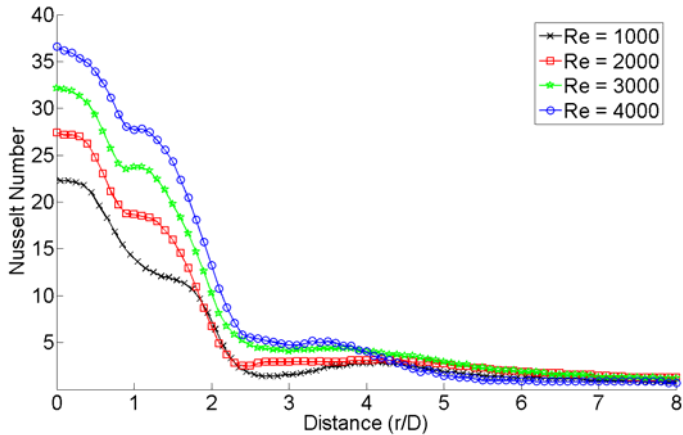


Figure 2b: Heat transfer distribution for a steady jet at $H/D = 1.0$

In the above graphs at an H/D of 1 the magnitude of the steady jet heat transfer rate is up to 3 times that of the synthetic jet; this is largely due to confinement and recirculation effects on the synthetic jet. Recirculation effects can be seen in figure 2a reaching a radial distance of approximately 2.2, this was shown by McGuinn et al. (2008) using Particle Image Velocimetry to confirm that these recirculation zones do exist for synthetic jets at an $H/D = 1$.

From a radial distance of 2.2 onwards in figure 2a the jet becomes confined.

Effects of recirculation can be seen in figures 2a and 2b, at an r/D of 3 to 4; this is thought to occur because of the way confinement affects synthetic and steady jets at low H/D values. This effect can be seen across the range of Reynolds numbers tested at this H/D for both the synthetic jet and the steady jet.

Although the steady jet has the same degree of geometric confinement, it is the lack of a fresh supply of cooling air in the confined synthetic jet case that explains its low heat transfer.

The results of figure 2a also suggest that synthetic jets are not as scalable with Reynolds numbers when highly confined as in less confined cases.

In figure 2b there is a transition to turbulence at a radial distance of approximately 1.2 this will explain the secondary peaks that are evident for the steady jet.

As the height of the jets above the impingement surface is increased there is less likelihood of confinement occurring, therefore allowing the jet to fully propagate, and maximum heat transfer to take place.

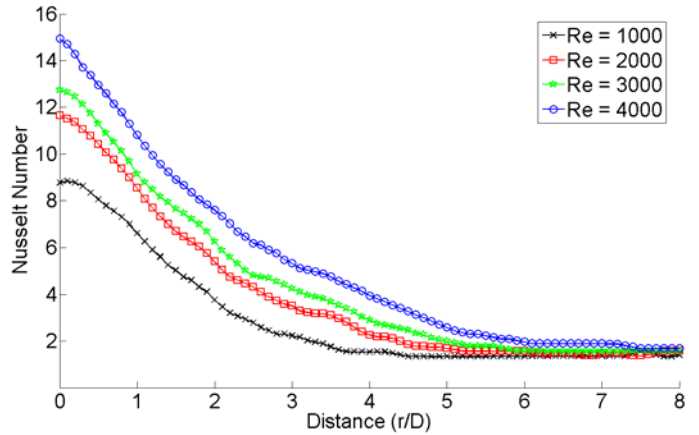


Figure 3a: Heat transfer distributions for a synthetic jet at $H/D = 2.0$

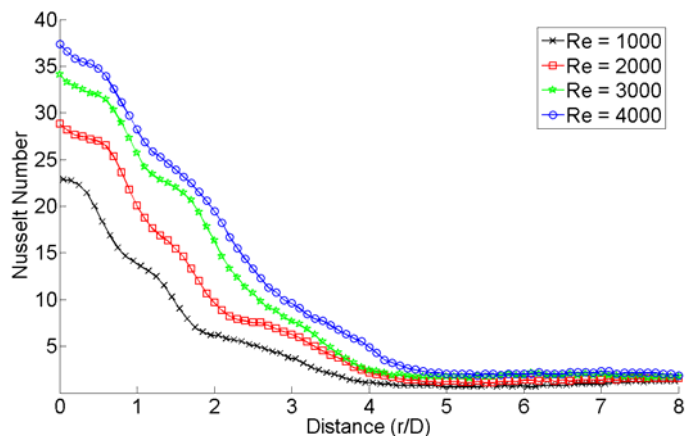


Figure 3b: Heat transfer distributions for a steady jet at $H/D = 2.0$

Comparing the above heat transfer profiles at an H/D of 2, it can be seen that the magnitude of the steady jet heat transfer rate is nearly double that of the synthetic jet.

The secondary peaks in figure 3b are reduced in comparison to the secondary peaks in figure 2b, this is partly due to the increase in H/D and the somewhat laminar flow region that begins to occur from $r/D = 1$.

In figure 3b the synthetic jet has already transitioned to turbulence, and there is quite a linear heat transfer distribution which is similar to the results for the synthetic jet at $H/D = 6$ in figure 4a. The clearly linear heat transfer distribution in figures 3a and 4a helps in illustrating the effects that confinement and recirculation have on synthetic jets because there is a much more linear heat transfer distribution than that in figure 2a.

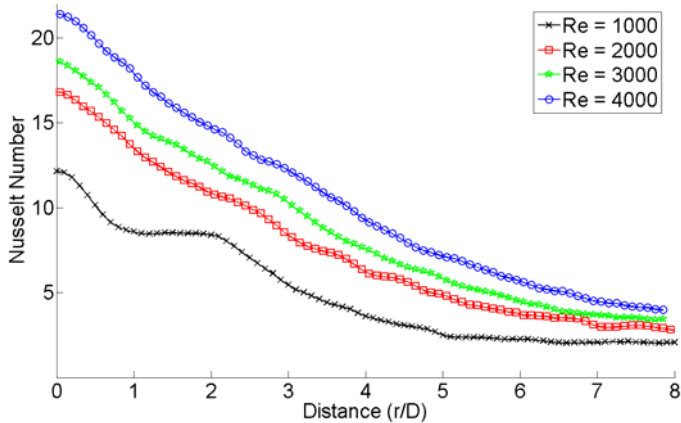


Figure 4a: Heat transfer distributions for a synthetic jet at $H/D = 6.0$

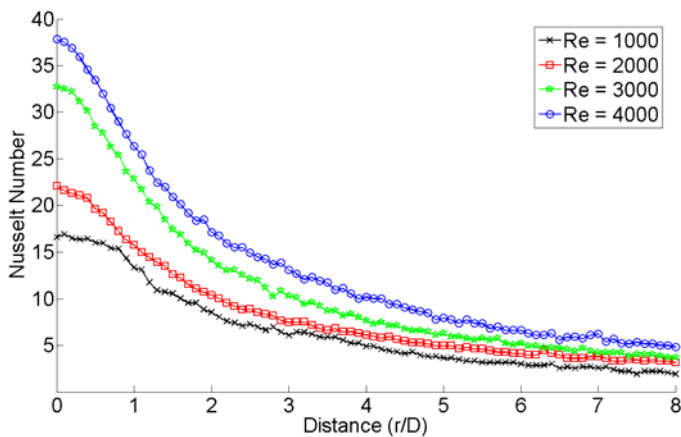


Figure 4b: Heat transfer distributions for a steady jet at $H/D = 6.0$

At $H/D = 6$ the effects of confinement on the synthetic jet is not as apparent as it is in lower H/D values, as can be seen in figure 4a. In this case, the magnitude of the steady jet is approximately 1.5 times that of the synthetic jet.

In figure 4b there is clearly no secondary peaks and the Nusselt numbers reduce uniformly with increasing r/D , this is due to the higher jet to plate spacing allowing there to be a more laminar flow. It can be seen at the Reynolds number of 1000 the Nusselt number is significantly lower than all the other steady jet results, because it is a higher H/D there appears to be a loss of momentum which could be due to a diminished core.

With regard to synthetic jets it is worth noting that as the height above the plate is increased the recirculation effect is reduced. It was demonstrated by McGuinn et al. (2008) that at $H/D = 1$ there exist strong recirculation zones on either side of the jet. This can be clearly seen in figure 2a at a radial distance

of 1.8. Although these recirculation zones still exist at $H/D = 2$ it was found by McGuinn et al. (2008) that there is far more entrainment, there is evidence to suggest that this trend increases up to $H/D = 10$, as reported by Gillespie et al. (2006).

Although the steady jet performs better in this study, some aspects of synthetic jets are beneficial to heat transfer:

1. The stronger entrainment of surrounding fluid
2. The vigorous mixing near the impingement surface, periodically breaking up the thermal boundary layer.

The above aspects are mostly contained in the near field. From a heat transfer point of view, the far field is therefore not really of interest.

CONCLUSION

The Nusselt numbers for a steady jet and a synthetic jet differ strongly at low Reynolds numbers and low H/D , with the difference reducing as the degree of confinement is reduced. In all cases the steady jet yields higher Nusselt number.

At low H/D values the effects of recirculation, albeit small, can be seen at $H/D = 1$ for synthetic and steady jets; this is largely due to the low jet to plate spacing.

Higher Reynolds numbers produced greater heat transfer rates, for both steady jet and synthetic jet, as anticipated.

It is apparent that for steady jets the mean Nusselt number is highly dependent on jet Reynolds number. Results here show that this is not the case for synthetic jets where very similar heat transfer is achieved at $H/D = 1$ for the Reynolds numbers of 3000, 4000 (figure 2a).

The observed trends in the heat transfer profiles for different jet to plate spacings indicate that confinement affects steady jets less than synthetic jets at low H/D values.

The effectiveness of synthetic jets depends on several factors, one being the dimensionless stroke length (L_o/D), this study was completed utilising a dimensionless stroke length (L_o/D) for the synthetic jet held constant at 8. Varying the dimensionless stroke length will undoubtedly have a direct effect on the heat transfer rates of the synthetic jets.

Future work in this area will include a study of the effect of varying the dimensionless stroke length with a constant Reynolds number, and measuring fluctuating heat transfer.

ACKNOWLEDGMENTS

The authors acknowledge the technical support staff of the Mechanical and Manufacturing Engineering Department of Trinity College.

The project is part funded by Science Foundation Ireland (SFI) in collaboration with the Centre for Telecommunications Value-Chain Research (CTVR).

REFERENCES

- Persoons T, O'Donovan T. S. (2007) A pressure-based estimate of synthetic jet velocity. *Physics of Fluids* 19(12):128104.
- Smith B. L., Glezer A (1998) The formation and evolution of synthetic jets. *Physics of Fluids* 10:2281-2297.
- Kercher D. S., Lee J. B., Brand O., Allen M. G., Glezer A., (2003) Microjet cooling devices for thermal management of electronic, *J. Chem. Theory Comput.*, 26_2_, pp. 359-366.
- Glezer A., Amitay M., (2002) Synthetic Jets, *Annual reviews Fluid Mechanics*, pp. 503-634.
- Liu T., Sullivan, J. P., (1996) Heat transfer and flow structures in an excited circular impinging jet, *International Journal of Heat and Mass Transfer*, 39, pp. 3695-3706.
- T. S. O'Donovan and D. B. Murray, "Jet impingement heat transfer - Part I: Mean and root-mean-square heat transfer and velocity distributions," *International Journal of Heat and Mass Transfer*, vol. 50, pp. 3291-3301, 2007.
- Lytle D., Webb B. W., (1994) Air jet impingement heat transfer at low nozzle-plate spacings. *International Journal of Heat and Mass Transfer*, 37, pp. 1687-1697.
- McGuinn A., Persoons T., Valiorgue P., O'Donovan T. S., Murray D. B., (2008) Heat transfer measurements of an impinging synthetic air jet with constant stroke length. Eurotherm, 5th European Thermal-Sciences Conference
- Gillespie M., Black W., Rinehart C., Glezer A., (2006) Local convective heat transfer from a constant heat flux plate cooled by synthetic air jets, *ASME Journal of Heat Transfer*, Vol. 128